# A Drag free control based on Model Predictive Technics

David Prieto
Dipartimento di Automatica ed Informatica
Politecnico di Torino
Torino, Italy
Email: luis.prieto@polito.it

Zuheir Ahmad
Dipartimento di Automatica ed Informatica
Politecnico di Torino
Torino, Italy
Email: zuheir.ahmad@polito.it

*Abstract*— **This paper presents a solution for the drag free control problem of the European satellite GOCE based on Model Predictive technics. The approach followed during the orbit and attitude modelling yields to the decoupling of the plant's six degrees of freedom into four linearized systems that include satellite's dynamics, sensors and its corresponding noise profiles, actuators and its relative noise profiles and also, the characterization of the main exogenous disturbances (drag forces and torques). In the problem formulation are considered performance constrains in terms of the propulsion system activity, residual acceleration levels (linear and angular) and the spacecraft's attitude angles. Also, it is presented the process to traduce the orbit and attitude performance requirements into specific mathematical constraints for the calculation of the optimal control law by means of predictive techniques. Simulation results using atmospheric drag profiles validated for this mission by Alenia Spazio (main mission contractor), are presented and analyzed in order to confirm the fulfilment of constraints and the performance requirements achieving.**

## I. INTRODUCTION

The Gravity Field and Ocean Circulation Explorer (GOCE) is a mission of the European Space Agency (ESA) oriented to the extremely high accurate measuring of the Earth's gravity field (less than $10\mu m/s^2$) and the geoid modelling (accuracy of $1-2cm$) at a spatial resolution better than $100km$ [1]. The mission will be developed with a single rigid octagonal spacecraft of approximately $5m$ long and $1m$ in diameter with fixed solar wings and no moving parts. In order to reach high accuracy in the determination of the lower harmonics of the gravity field, Precise Orbit Determination (POD) is implemented through a 12-channel GPS receiver with geodetic quality. Complementary, the measurement of medium and high harmonics of the gravity field ($0.005Hz \leq f \leq 0.1Hz$) is developed through Satellite Gravity Gradiometry (SGG). This technic uses an ensemble of three pairs of three-axial electrostatic accelerometers (gravity gradiometers), each one containing a $320g$ proof mass electrostatically suspended and mechanically isolate from the spacecraft's main body through a specially engineered cage. The specific role of the Drag Free Control (DFC) for the GOCE can be defined as an advanced drag compensation system that keeps the six proof masses in near 'free fall motion' and the average orbital altitude at about $250km$. To develop these tasks, the forces that maintain each proof mass at the center of the cage are measured and the deviation from the nominal position within the allowed clearance band is used by the control system for commanding the propulsion system (two ion propulsion thruster and eight cold gas thrusters), that compensates the non-gravitational disturbance forces. The GOCE is thus forced to chase the proof masses, actively shielding it from the non-gravitational forces, the largest of which is the atmospheric drag. In this way, the complementary use of POD and SGG provide data sets of gravity gradient components with enhanced quality, respect to traditional techniques that have already reached their intrinsic limits [2].

Although, it is not a new problem, new realizations have been made in the last years integrating modern control techniques such $\mathcal{H}_\infty/\mathcal{H}_2$ [3], [4] and Embedded Model Control [2], [5] as valid means for improving stability and performance robustness of the DFC control. Nevertheless, the $\mathcal{H}_\infty$ formulation [3], [4] may not always achieve optimal performance, from the propulsion system point of view, when the worst-case plant (base assumption of these techniques) rarely or never occurs. On the other hand, in [5], is well described the difficult tradeoff between minimization of thrust level and achieving performance requirements at low frequency. In fact, not all the specifications for the GOCE Drag Free Control are satisfied in [5] at low frequencies as a payload for a low command activity.

In this frame, the aim of this paper is to solve the DFC problem for the European mission Gravity Field and Steady-State Ocean Circulation Explorer (GOCE) [1], showing that a Model Predictive approach allows the inclusion in the design of most restrictive constraints that conduct to a reduction of the propulsion system activity respect to other modern alternatives [3], [4]. Also, it is presented the process to traduce the orbit and attitude performance requirements into specific mathematical constraints for the calculation of the optimal control law by means of predictive techniques. Simulation results using atmospheric drag profiles validated for this mission by Alenia Spazio (main mission contractor), are presented and analyzed in order to confirm the fulfilment of constraints and the performance requirements achieving.

## II. Mathematical model

### A. Reference frames

For establishing the mathematical model of GOCE's motion, it is necessary to define a set of coordinate systems that allow a correct and easy integration of all the phenomena involved:

*1) Inertial reference frame (IRF):* For practical purposes, a geocentric coordinate system is a suitable IRF due to the almost circular and unaccelerated motion of the Earth around the sun (orbit period $> 365$ days) [6]. Based on this consideration, it is defined an IRF with origin at the Earth's Center of Mass (CoM); the $Z_{j2000}$ axis, is the axis of Earth's rotation that intersects the celestial sphere at the north celestial pole; the $X_{j2000}$ axis coincides with the vernal equinox vector (at the epoch January $1, 2000$); the $Y_{j2000}$ axis completes the right-handed orthogonal coordinate system.

*2) Local Orbit Reference Frame (LORF):* It is a non-inertial reference frame used for describing the drag forces that perturbate the LEO. The origin is placed in the CoM of the spacecraft; the $X_L$ axis is parallel to the instantaneous orbital velocity vector ($\boldsymbol{v}$); the $Y_L$ axis is parallel to the instantaneous direction of the orbit angular momentum ($\boldsymbol{h} = \boldsymbol{r} \times \boldsymbol{v}$); the $Z_L$ axis completes the right-handed orthogonal coordinate system.

*3) Spacecraft Reference Frame (SCRF):* It is a non-inertial reference frame used for describing the spacecraft attitude dynamics. The origin is placed in the CoM of the spacecraft; its $\boldsymbol{i_s}$ points toward the motion direction; $\boldsymbol{k_s}$ is orthogonal to the satellite earth face (positive direction is towards nadir); the $\boldsymbol{j_s}$ axis completes the right-handed orthogonal coordinate system.

*4) Natural Orbit Reference Frame (NORF):* It is a non-inertial reference frame, suitable for the deduction of a space state model that describes the physical phenomena in terms of orbit plane (nominal case) and out-of-plane dimensions. The origin is placed in the Earth's Center of Mass; the $X_n$ axis points toward the perigee in the orbit plane; the $Y_n$ axis is parallel to the instantaneous direction of the orbit angular momentum ($\boldsymbol{h} = \boldsymbol{r} \times \boldsymbol{v}$); the $Z_n$ axis completes the right-handed orthogonal coordinate system. The transformation from NORF to IRF is provided through the following transformation matrix:

$$\begin{bmatrix} \boldsymbol{X_j} \\ \boldsymbol{Y_j} \\ \boldsymbol{Z_j} \end{bmatrix} = \begin{bmatrix} \boldsymbol{R_z}(-\boldsymbol{\Omega})\boldsymbol{R_x}(-\boldsymbol{i})\boldsymbol{R_z}(-\boldsymbol{\omega}) \end{bmatrix} \begin{bmatrix} \boldsymbol{X_N} \\ \boldsymbol{Y_N} \\ \boldsymbol{Z_N} \end{bmatrix} \quad (1)$$

Specifically in (1), the $Z_N$ axis is first rotate clockwise by the argument of the perigee ($\omega$), aligning the original $X_N$ axis with the line of nodes. Then, the X axis of this new coordinate system is rotated clockwise by the inclination angle ($i$), aligning the orbit plane with the Earth's Equatorial plane. Finally, the Z axis of this new coordinate system is rotated clockwise by the right ascension of the ascending node ($\Omega$). The transformation from LORF to IRF is provided through the following rotation matrix:

$$\begin{bmatrix} \boldsymbol{X_j} \\ \boldsymbol{Y_j} \\ \boldsymbol{Z_j} \end{bmatrix} = \begin{bmatrix} \frac{\boldsymbol{v}}{\|\boldsymbol{v}\|} & \frac{\boldsymbol{v}\times\boldsymbol{r}}{\|\boldsymbol{v}\times\boldsymbol{r}\|} & \frac{\boldsymbol{v}\times\boldsymbol{r}\times\boldsymbol{v}}{\|\boldsymbol{v}\times\boldsymbol{r}\times\boldsymbol{v}|} \end{bmatrix} \begin{bmatrix} \boldsymbol{X_L} \\ \boldsymbol{Y_L} \\ \boldsymbol{Z_L} \end{bmatrix} \quad (2)$$

where, $\boldsymbol{v}$ and $\boldsymbol{r}$ are the instantaneous velocity and position vectors respectively. The transformation from the LORF to the SCRF, assuming an active attitude control, is provided through the following matrix:

$$\begin{bmatrix} \boldsymbol{X_s} \\ \boldsymbol{Y_s} \\ \boldsymbol{Z_s} \end{bmatrix} = \begin{bmatrix} 1 & \psi & -\theta \\ -\psi & 1 & \phi \\ \theta & -\phi & 1 \end{bmatrix} \begin{bmatrix} \boldsymbol{X_L} \\ \boldsymbol{Y_L} \\ \boldsymbol{Z_L} \end{bmatrix} \quad (3)$$

where, $\phi$, $\theta$ and $\psi$ are the roll, pitch and yaw angles.

### B. Orbit dynamics

Representing the position vector as $\boldsymbol{r} = r\boldsymbol{e_r}$, then the linear velocity vector ($\boldsymbol{v} = \dot{\boldsymbol{r}}$) and the linear acceleration ($\boldsymbol{v} = \ddot{\boldsymbol{r}}$) in the NORF are:

$$\begin{aligned} \boldsymbol{r} &= r\boldsymbol{e_r} && (4) \\ \dot{\boldsymbol{r}} &= \dot{r}\boldsymbol{e_r} + r\dot{\boldsymbol{e}}_{\boldsymbol{r}} = \dot{r}\boldsymbol{e_r} + (r\dot{\theta}\cos\phi)\boldsymbol{e_\theta} + \dot{\phi}\boldsymbol{e_\phi} && (5) \\ \ddot{\boldsymbol{r}} &= \ddot{r}\boldsymbol{e_r} + \dot{r}\dot{\boldsymbol{e}}_{\boldsymbol{r}} + (\dot{r}\dot{\theta}\cos\phi + r\ddot{\theta}\cos\phi - r\dot{\theta}\dot{\phi}\sin\phi)\boldsymbol{e}_\theta + \\ &\quad r\dot{\theta}\cos\phi\dot{\boldsymbol{e}}_\theta + (\dot{r}\dot{\theta} + r\ddot{\phi})\boldsymbol{e}_\phi + r\dot{\phi}\dot{\boldsymbol{e}}_{\boldsymbol{\phi}} \\ \ddot{\boldsymbol{r}} &= (\ddot{r} - r\dot{\theta}^2\cos^2\phi - r\dot{\phi}^2)\boldsymbol{e}_r + \\ &\quad (r\ddot{\theta}\cos\phi + 2\dot{r}\dot{\theta}\cos\phi - 2r\dot{\theta}\dot{\phi}\sin\phi)\boldsymbol{e}_\theta && (6) \\ &\quad + (r\ddot{\phi} + 2\dot{r}\dot{\phi} + r\dot{\theta}^2\sin\phi\cos\phi)\boldsymbol{e}_\phi \end{aligned}$$

In order to deduce the complete dynamic description of the system, the force model (4)-(6) is complemented with the vector of perturbation forces ($d_i$), the residual terms (zonal and tesseral harmonics) of the gravitational model ($g_i$), and the vector of control variables ($u_i$) to be applied by the propulsion subsystem:

$$\ddot{r} - r\dot{\theta}^2\cos^2\phi - r\dot{\phi}^2 + \frac{\mu_\oplus}{r^2} = \frac{d_r}{m} + g_r + \frac{u_r}{m} \quad (7)$$

$$r\ddot{\theta}\cos\phi + 2\dot{r}\dot{\theta}\cos\phi - 2r\dot{\theta}\dot{\phi}\sin\phi = \frac{d_\theta}{m} + g_\theta + \frac{u_\theta}{m} \quad (8)$$

$$r\ddot{\phi} + 2\dot{r}\dot{\phi} + r\dot{\theta}^2\sin\phi\cos\phi = \frac{d_\phi}{m} + g_\phi + \frac{u_\phi}{m} \quad (9)$$

where, $m$ represents the mass of the spacecraft. The orbit of the GOCE is characterized for: a near-polar trajectory (Figure 1(b)), a low eccentricity ($< 0,005$, Figure 1(c)), a high inclination angle ($96.5^o$, Figure 1(d)), a mean altitude ($r_o$) of $250km$ and a quasi constant angular velocity ($\omega_o$) of $1,17mrad/s$ [1]. Considering these conditions as a nominal scenario and developing the corresponding linearization of the system of equations (7)-(9), the satellite's orbit dynamics can be approximated through the following linearized

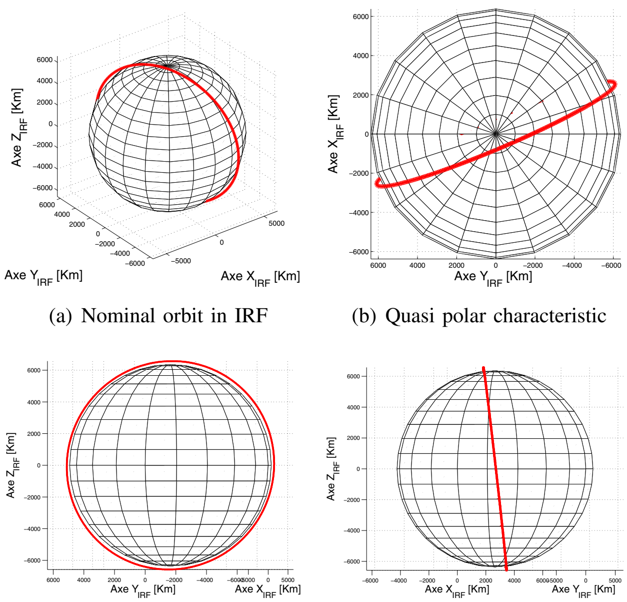


(a) Nominal orbit in IRF

(b) Quasi polar characteristic

(c) Circular form

(d) Inclination angle

Fig. 1. Simulation results evidencing nominal orbit characteristics

orbit relative motion model:

$$\begin{bmatrix} \dot{\hat{x}}_o \\ \ddot{\hat{x}}_o \\ \dot{\hat{y}}_o \\ \ddot{\hat{y}}_o \\ \dot{\hat{z}}_o \\ \ddot{\hat{z}}_o \end{bmatrix} = \begin{bmatrix} 0 & 1 & 0 & 0 & 0 & 0 \\ 3\omega_o^2 & 0 & 0 & 2\omega_o & 0 & 0 \\ 0 & 0 & 0 & 1 & 0 & 0 \\ 0 & -2\omega_o & 0 & 0 & 0 & 0 \\ 0 & 0 & 0 & 0 & 0 & 1 \\ 0 & 0 & 0 & 0 & -\omega_o^2 & 0 \end{bmatrix} \begin{bmatrix} \hat{x}_o \\ \dot{\hat{x}}_o \\ \hat{y}_o \\ \dot{\hat{y}}_o \\ \hat{z}_o \\ \dot{\hat{z}}_o \end{bmatrix} + \tag{10}$$

$$\begin{bmatrix} 0 & 0 & 0 \\ \frac{1}{m} & 0 & 0 \\ 0 & 0 & 0 \\ 0 & \frac{1}{m} & 0 \\ 0 & 0 & 0 \\ 0 & 0 & \frac{1}{m} \end{bmatrix} \begin{bmatrix} \hat{d}_{xo} \\ \hat{d}_{yo} \\ \hat{d}_{zo} \end{bmatrix} + \begin{bmatrix} 0 & 0 & 0 \\ \frac{1}{m} & 0 & 0 \\ 0 & 0 & 0 \\ 0 & \frac{1}{m} & 0 \\ 0 & 0 & 0 \\ 0 & 0 & \frac{1}{m} \end{bmatrix} \begin{bmatrix} \hat{u}_{xo} \\ \hat{u}_{yo} \\ \hat{u}_{zo} \end{bmatrix}$$

where, $x_o$, $y_o$ and $z_o$ are the components of the relative orbit motion vector described into a non inertial reference frame with origin at the GOCE's CoM; the $Y_o$ axis is parallel to the instantaneous orbital velocity vector ($\boldsymbol{v}$); the $Z_o$ axis is parallel to the instantaneous direction of the orbit angular momentum ($\boldsymbol{h} = \boldsymbol{r} \times \boldsymbol{v}$); the $X_o$ axis completes the right-handed orthogonal coordinate system as described in Figure 2. It is important to remark that residual gravitational terms are not included into the perturbations to be rejected, because the GOCE mission is oriented to measured such gravity anomalies. An analysis of (10), shows that the orbit plane dynamics and the NORF declination coordinate are decoupled. This means that motion in the orbit plane can be considered separately from the out-of-plane dynamics. The controllability (stabilizability) and observability (detectability) analysis, reveals a complete controllability of the orbit plane dynamics from the tangent component ($u_{yo}$). This is an important aspect to be assessed in a later treatment of balanced thrusters function and in the optimization of the satellite's propulsion system.

### C. Attitude model

The Euler's equation of motion, in the SCRF, for the GOCE can be expressed as:

$$I_x\dot{\omega}_x - (I_y - I_z)\omega_y\omega_z = u_x + T_x \tag{11}$$

$$I_y\dot{\omega}_y - (I_z - I_x)\omega_z\omega_x = u_y + T_y \tag{12}$$

$$I_z\dot{\omega}_z - (I_x - I_y)\omega_x\omega_y = u_z + T_z \tag{13}$$

where, $I_x, I_y, I_z$ are the principal moments of inertia, $\omega_x, \omega_y, \omega_z$ are the SCRF components of the satellite's absolute angular velocity, $u_i$ are the control torques applied by the attitude controller and $T_i$ are the exogenous torques due to non-gravitational forces (gravity gradient, Earth Magnetic Field, atmospheric drag). For small attitude deviation from the LORF orientation, the following linear relations can be applied:

$$\omega_x = \dot{\phi} - \omega_o\psi \tag{14}$$

$$\omega_y = \dot{\theta} - \omega_o \tag{15}$$

$$\omega_z = \dot{\psi} + \omega_o\phi \tag{16}$$

Using (14)-(16) into (11)-(13) and considering also the gravity gradient effect [6], the linear equations for rotational motion in the SCRF can be described as:

$$I_x\ddot{\varphi} - \omega_o(I_x - I_y + I_z)\dot{\psi} + 4\omega_o^2(I_y - I_z)\varphi = T_x + u_x \tag{17}$$

$$I_y\ddot{\theta} + 3\omega_o^2(I_x - I_z)\theta = T_y + u_y \tag{18}$$

$$I_z\ddot{\psi} + \omega_o(I_x - I_y + I_z)\dot{\varphi} + \omega_o^2(I_y - I_x)\psi = T_z + u_z \tag{19}$$

An analysis of (17)-(19), shows that the pitch dynamics are decoupled from the roll/yaw dynamics, so the respective controllers can be synthesized separately.

### D. Sensor modelling

The gradiometer bandwidth is about $1Hz$, with a damping coefficient of 0.7 and a steady state gain asymptotically equal to 1. The measurement noise introduced in the control system by the gradiometer can be considered as a white noise with a spectral density of approximately $3.7810 - 11rad/s^2$ [3].

### E. Propulsion subsystem

The thrusters used to applied the forces required for orbit and attitude drag compensation are characterized for a second order behavior with a bandwidth of 20 Hz and damping coefficient of 0.7. The noise introduced into the control system by each thruster can be considered as a white noise with a spectral densities around $4.610-4rad/s^2$ ($u_x$), $6.610 - 4rad/s^2$ ($u_y$), $1.810 - 3rad/s^2$ ($u_z$)) [3]

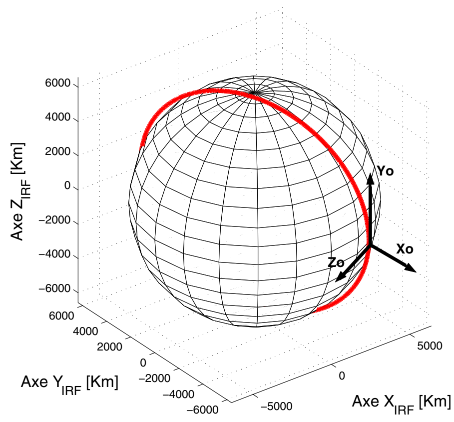


Fig. 2. Auxiliary Local Orbit Reference Frame (ALORF)

TABLE I
PERFORMANCE REQUIREMENTS FOR GOCE MISSION

| Variable (units) | Symbol | $f <$ 5mHz | MBW | $f >$ 0.1Hz |
|---|---|---|---|---|
| Linear accel. | $X_o$ | 0.1 | 0.025 | 0.5 |
| in ALORF | $Y_o$ | 0.1 | 0.025 | 0.5 |
| $(\mu m/s^2\sqrt{Hz})$ | $Z_o$ | 0.5 | 0.025 | 0.1 |
| Angular | $\dot{\omega}_x$ | 1 | 0.024 | 1 |
| accelerations | $\dot{\omega}_y$ | 1 | 0.024 | 1 |
| $(\mu rad/s^2\sqrt{Hz})$ | $\dot{\omega}_z$ | 1 | 0.024 | 1 |
| Attitude | $\phi$ | 26000 | 7.9 | NA |
| angles | $\theta$ | 26000 | 7.9 | NA |
| $(rad/\sqrt{Hz})$ | $\psi$ | 26000 | 7.9 | NA |

## III. MODEL PREDICTIVE CONTROL ALGORITHM

### A. Control specifications

Once defined the DFC as a relative motion problem, the main performance requirements are established from the mission specifications. In particular, the techniques for gravity field determination on the GOCE mission (precise Orbit Determination, GPS /GLONASS orbit monitoring to cm-precision, and gravity gradiometry) determine that PSD of satellite incremental accelerations and attitude angles should be kept below the values specified in Table I (see [1], [3], [2]). Also, the propulsion technology considered (Ion thrusters and microthrusters), limits the amplitude of control forces to the values shown in Table II (see [2]).

TABLE II
THRUSTERS PEAK FORCES $(mN)$ AND TORQUES $(nNm)$

| $\hat{U}_{xo}$ | $\hat{U}_{yo}$ | $\hat{U}_{zo}$ | $U_x$ | $U_y$ | $U_z$ |
|---|---|---|---|---|---|
| 1.15 | 20.5 | 0.57 | 0.24 | 0.18 | 0.32 |

### B. Model Predictive Control (MPC) approach

As indicated in the model analysis of section II-B, four MIMO systems have to be controlled: two, related with the orbit modelling ($X_o$-$Y_o$, $Z_o$) and the other two, related with the attitude characterization ($\phi-\psi$, $\theta$ ). The MPC method applied is the same for all cases and consist of a fixed horizon algorithm with a quadratic cost function. The finite prediction horizon ($N_p$) is a relevant concept into this problem because it allows to minimize the performance measure through an optimization problem with a finite number of decision variables and a finite number of constraints directly related with the orbit and performance requirements. From the control point of view, good disturbance rejection requires a high bandwidth but in the presence of sensor noise, higher controller bandwidth results in transmission of sensor noise into larger thrust usage. This stochastic balance of demands is satisfied optimally by a quadratic cost function. In this way, at each sampling time, starting at the current state, the optimal control problem is solved over a finite horizon. The optimal command signal is applied to the GOCE propulsion system only during the immediately following sampling interval. At the next time step a new optimal control problem based on new measurements of the state is solved over a shifted horizon. From a mathematical point of view, the problem is posed as to find the optimal control signal ($\hat{u}_i$ or $u_i$) that minimizes the following finite horizon performance cost function:

$$\min_{U} \mathbf{J}(U, x(t|t), N_p, N_c) \tag{20}$$

subject to: $LU \leq K$ and $TU \leq Z$
where:

$$\mathbf{J} = \sum_{k=0}^{N_p-1} x_{t+k|t}^T Q x_{t+k|t} + \sum_{k=0}^{N_c-1} u_{t+k|t}^T R u_{t+k|t}$$

$N_p$ is the prediction horizon
$N_c$ is the control horizon ($N_c \leq N_p$)

$$u_{t+k|t} = u_{t+N_c-1|t} \; k = N_c, N_c+1, \cdots, N_p-1$$

$$U = \left(u_{t|t}^T, u_{t+1|t}^T, \cdots, u_{t+N_c-1|t}^T\right)$$

$Q = Q^T \succ 0$ and $R = R^T \succ 0$(the performance weights).

The variables $x_{t+k|t}$ denote predicted states, given an input sequence $u_{t+k|t}$, a state estimate $x_{t|t}$ and considering a discrete space state model of the system.

### C. Quadratic Programming Formulation of MPC

Due to the quadratic property of the performance objective $\mathbf{J}$ and in the presence of constraints on the control variables and the system states, the optimization problem in (20) can be transformed into a constrained quadratic programming problem [7] with consequent well known and efficient solution methods. To put the optimization problem in a form suitable for quadratic programming, there are introduced stacked vectors with future states and outputs:

$$X = \left(x_{t|t}^T, x_{t+1|t}^T, \cdots, x_{t+N_p-1|t}^T\right)^T \tag{21}$$

From a discrete state space representation, the k-step ahead prediction of the system states and outputs can be written as:

$$x_{t+k|t} = A^k x_{t|t} + \sum_{i=0}^{k-1} A^i B u_{t+k-1-i|t} \quad k = 1, 2, \cdots, N_p - 1 \tag{22}$$

Consequently the predicted states can be expressed as:

$$X = \Omega x_{t/t} + \Gamma U \tag{23}$$

where $\mathcal{C} = diag(C, \cdots, C) \in \mathbf{R}^{N_p \cdot p \times N_p \cdot n}$ and $\Omega$ ,$\Gamma$ are given by

$$\Omega = \begin{pmatrix} I \\ A \\ A^2 \\ \vdots \\ A^{N_p-1} \end{pmatrix} \quad \Gamma = \begin{pmatrix} 0 & 0 & 0 & \cdots & 0 \\ B & 0 & 0 & \cdots & 0 \\ AB & B & 0 & \cdots & 0 \\ \vdots & & \ddots & \ddots & \vdots \\ A^{N_p-2}B & A^{N_p-3}B & \cdots & B & 0 \end{pmatrix}$$

The cost function $\mathbf{J}$ can be articulated as:

$$\mathbf{J}(U, X) = X^T \mathcal{Q} X + U^T \mathcal{R} U \tag{24}$$

where,

$$\mathcal{Q} = diag(Q, \cdots, Q) \quad \mathcal{R} = diag(R, \cdots, R)$$

Using (23) the cost function becomes:

$$\mathbf{J} = \frac{1}{2} U^T \mathbf{H} U + \mathbf{F}^T U \tag{25}$$

where,

$$\mathbf{H} = 2\left(\Gamma^T \mathcal{Q} \Gamma + \mathcal{R}\right) \quad \mathbf{F} = 2 x_{t|t}^T \Omega^T \mathcal{Q} \Omega$$

### D. Constraint handling

To ensure the stability of the control law obtained using MPC algorithm , it is impose the terminal constraint that the state vector $x_{t+N_p|t}$:

$$A^{N_P} x_{t|t} + \sum_{i=0}^{N_p-1} A^i B u_{t+N_p-1-i|t} = 0 \tag{26}$$

which can be written as $TU = Z$ where,

$$Z = -A^{N_P} x_{t|t}$$

$$T = \left(A^{N_p-1}B, A^{N_p-2}B, \cdots, B\right)$$

The constraints imposed on the control variables when optimizing (20) will be the following:

$$-u_{max} \le u_{t+k|t} \le u_{max} \qquad k = 0, 1, \cdots, N_c - 1 \tag{27}$$

where $U_{max}$ is a column vector containing the maximum values of control variables (Table II). The constraints imposed to the output variables are expressed as:

$$-y_{max} \le y_{t+k|t} \le y_{max} \qquad k = 0, 1, \cdots, N_p - 1 \tag{28}$$

where $Y_{max}$ is a column vector containing the maximum values of output variables (Table II). Equations 27 and 28

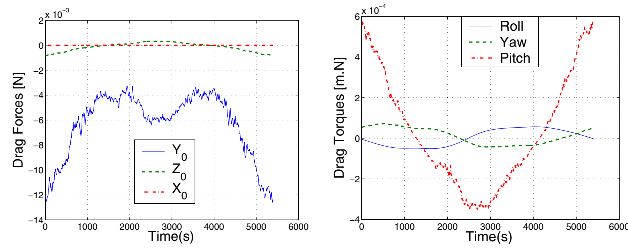


(a) Atmospheric drag forces $\hat{d}_{io}$ (b) Atmospheric drag torques $d_i$

Fig. 3. Atmospheric drag profiles for GOCE mission

can be written as linear constraints on $U$ of the form $LU \le K$, where

$$L = \begin{pmatrix} I_d \\ -I_d \\ \Phi \\ -\Phi \end{pmatrix} \quad K = \begin{pmatrix} U_{max} \\ -U_{max} \\ Y_{max} \\ -Y_{max} \end{pmatrix}$$

and $I_d = diag(I, \cdots, I)$ is a $N_c \cdot m \times N_c \cdot m$ matrix and $I$ is the $m \times m$ identity matrix (where $m$ is the number of input variables). $\Phi$ is a matrix with dimensions $p \cdot m \cdot N_p \times N_c \cdot m$ (where $p$ is the number of system outputs) and is equal to:

$$\Phi = \begin{pmatrix} CB & 0 & 0 & \cdots & 0 \\ CAB & CB & 0 & \cdots & 0 \\ CA^2B & CAB & CB & \cdots & 0 \\ \vdots & \vdots & \ddots & \ddots & \vdots \\ CA^{N_p-2}B & CA^{N_p-3}B & \cdots & CAB & CB \end{pmatrix}$$

The optimal solution can be numerically computed via the following optimization problem:

$$U^{opt} = arg \min_{\substack{LU \le K \\ TU = Z}} \mathbf{J}(U)$$

This is a convex problem due to the quadratic cost and linear constraints [7].

## IV. Simulation Results

The atmospheric drag profiles used for testing the MPC 4 were provided by Alenia Spazio (main contractor of the GOCE) and correspond to a highly accurate simulations of the expected disturbances during the mission work time. The MPC algorithm is applied to the four respective discrete systems, using the mission sampling time ($T = 0.1s$) [5], the constraint values indicated in Tables I and II and the procedure described in section III-D. The Q and R matrices are selected considering the results of the controllability analysis (section II-B). The best values that satisfy a trade off between performance requirements (attenuation factor in the bandwidth) and propulsion system activity are:

$$Q = \begin{bmatrix} 1 & 0 & 0 \\ 0 & 1 & 0 \\ 0 & 0 & 10^8 \end{bmatrix} \quad R = 10^{-10} \begin{bmatrix} 1 & 0 \\ 0 & 1 \end{bmatrix} \tag{29}$$

The prediction and control horizons are selected taking into account the nominal orbit requirements (period $\cong 90min$) and the sample time $(0, 1s)$. Specifically, with a $N_p = N_c = 20$, the number of parameters to optimize is

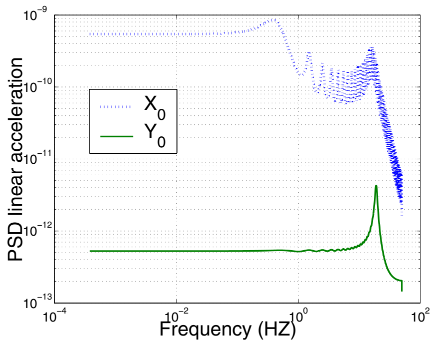


(a) PSD Orbit plane accelerations

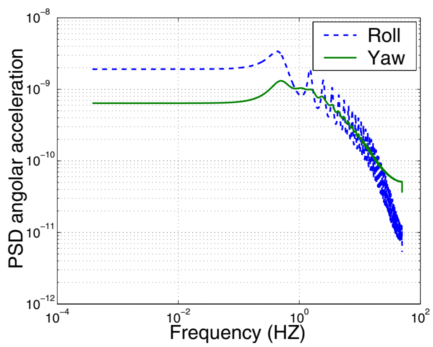


(b) PSD Roll and Yaw accelerations

Fig. 4. Power Spectral Density of residual orbit and attitude accelerations

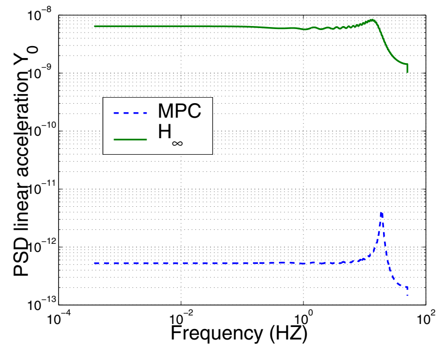


(a) Comparison of PSD results

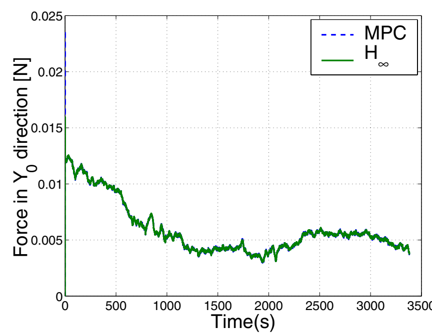


(b) Comparison of control signals

Fig. 5. Results comparison between MPC and a $\mathcal{H}_\infty$ controller

consistent with feasible computation times for the GOCE mission. The quadratic constrained optimization problem was numerically solved using Matlab optimization ToolBox with final results as indicated below. The four controllers are designed with the above criteria and considering the dynamics and noise profiles for gradiometer and the spacecraft's thrusters. The main results are showed in Figures 4(a) and 4(b), demonstrating that requirements are met with a comfortable margin of robustness. In fact, one of the most critical specification is the level of the PSD in the residual acceleration along the velocity vector ($Y_o$ in the ALORF), that the MPC maintains $90dB$ under the established limit in the MBW. Comparatively, in Figure 5 are simultaneously presented the results obtained for the same acceleration variable ($Y_o$) with a $\mathcal{H}_\infty$ [4] and a MP controllers. It is evident that the MPC reaches better performance with a control signal of the same level of that generated by the $\mathcal{H}_\infty$ controller. The on-line computation difficulties related to the MPC law can be overcome by means of a "Fast" implementation of the MPC algorithm (FMPC) [8].

## V. Conclusions

In this paper is proposed a Drag Free Control (DFC) based on predictive techniques for the GOCE mission of the ESA. The main contributions are related with the model set up as a linear decoupled plants and the use of predictive techniques for stabilizing the system and reaching attenuation values upper the performance requirements. Results demonstrate a better performance than traditional methods (state feedback) and modern frequency-weighted synthesis techniques.

## Acknowledgments


This research was supported in part by funds of Ministero dell'Istruzione dell'Universita e della Ricerca under the Project "Robustness and optimization techniques for control of uncertain systems".


## References


[1] E. S. Agency, "Goce mission requirements document," ESA Publications Division, The Nederlands, Tech. Rep., 2000.

[2] E. Canuto, B. Bona, M. Indri, and G. Calafiore, "Drag freee control for the european satellite goce. part i: Modeling," in *Procedings of the 41st IEEE conference on Decision and Control Conference*, Las Vegas, USA, December 2002, pp. 1269–1274.

[3] B. Ziegler and M. Blanke, "Drag-free motion control of satellite for high precision gravity field mapping," in *Procedings of IEEE international conference on control applications*, Glasgow, Scotland, U.K, september 2002.

[4] D. Prieto and B. Bona, "A modern approach to drag attenuation in a $\mathcal{H}_\infty$ robust orbit control," in *Proceedings of Procedings of IEEE International Conference in Information and Communication Technologies*, Damascus, Syria, Appril 2004.

[5] E. Canuto, B. Bona, M. Indri, and G. Calafiore, "Drag freee control for the european satellite goce. part ii: Digital control," in *Procedings of the 41st IEEE conference on Decision and Control Conference*, Las Vegas, USA, December 2002, pp. 4072–4077.

[6] M. Sidi, *Spacecraft Dynamics and Control*. New York: Cambrigge University Press, 1997.

[7] A. Bemporad and M. Morari, "The explicit linear quadratic regulator for constrained systems," *Automatica*, vol. 38, pp. 3–20, 2002.

[8] M. Canale and M. Milanese, "A fast implementation of model predictive control techniques," in *16th IFAC world congress*, Prague, Czech Republic, 2005.